EEET ECOLOGICAL ENGINEERING & ENVIRONMENTAL TECHNOLOGY

Ecological Engineering & Environmental Technology, 2026, 27(7), 270–282
https://doi.org/10.12912/27197050/224164
ISSN 2719–7050, License CC-BY 4.0

Received: 2026.05.18
Accepted: 2026.06.15
Published: 2026.07.01

Long-term seepage analysis and machine learning prediction at the left bank of Ouizert dam, Algeria (1989–2026)

Djamel Bekhtiar[1*], Hassane N. Benfetta[1,2]

[1] Department of Agronomy, Faculty of Nature and Life Sciences, University of Mustapha Stambouli of Mascara, Mascara 29000, Algeria
[2] Vegetal Chemistry-Water-Energy Laboratory, University of Hassiba Benbouali, Chlef, Algeria
* Corresponding author's e-mail: d.bekhtiar@univ-mascara.dz

ABSTRACT

Foundation seepage is a recurring constraint on the storage performance of Algerian dams, and in a country where per-capita renewable water is among the world's lowest the losses carry direct economic weight. The left bank of the Ouizert dam (Mascara province) has leaked since first impoundment in 1989, at a long-term average near 10.42 hm³ per year. We assembled and quality-controlled the full daily record to April 2026, yielding 12,521 validated daily measurements after removing 740 physically implausible readings and 81 statistical outliers (6.2% of the raw record); to our knowledge this is the longest validated seepage series compiled for an Algerian dam. Periodic levels from fourteen left-bank piezometers (2009–2026) complement it. Reservoir level Granger-causes leakage at lags of one to six months ($p < 0.001$) while the reverse direction is far weaker, establishing a directional rather than merely correlative link. A segmented regression places the operational threshold at 430.0 m NGA (95% bootstrap CI 428.5–430.5 m), above which the leakage–level slope steepens roughly fourfold. A calibrated head–discharge analysis shows the flow to be markedly non-Darcian: discharge follows a power law $Q \propto H^n$ with exponent $n \approx 3.4$, and the exponent rises from about 2.9 below the threshold to about 3.9 above it, with fracture Reynolds numbers in the turbulent range. Four models predicted monthly leakage from reservoir and piezometric inputs, with lagged leakage withheld so the models had to learn the physical driver rather than exploit autoregressive continuity. Gradient boosting performed best on the 2019–2026 hold-out ($R^2 \approx 0.60$; RMSE ≈ 95 L/s), with random forest close behind ($R^2 \approx 0.58$); five-fold time-series cross-validation returned 0.68 ± 0.14 for both, and linear and support-vector regression failed with negative R^2. Mean decrease in impurity, SHAP, and permutation importance independently agree that three- and six-month moving averages of reservoir level dominate prediction, consistent with hydraulic memory of weeks to months. Split-conformal intervals quantify forecast uncertainty for operational use. Contrary to a simple intensification narrative, monthly leakage shows no statistically significant long-term increase once level is controlled for; the regime is episodic and level-driven. The framework transfers to other Algerian dams on fractured-rock foundations.

Keywords: Ouizert dam, seepage, piezometry, machine learning, gradient boosting, change-point detection, Granger causality, karstic foundation, Algeria.

INTRODUCTION

Algeria built most of its large dams in the second half of the twentieth century to supply a growing population under an arid to semi-arid climate. Of roughly seventy large dams in service, at least fifteen lose more than one million cubic metres a year to foundation leakage and six exceed five million (Remini, 2005; Benfetta et al., 2017). Where renewable water per head is already scarce, such losses are a matter of regional water security. Ouizert ranks among the worst affected.

Ouizert is a 60-m earth-fill dam on the Oued Sahouet in Mascara province, with a design capacity near 100 hm³. It supplies drinking water to Oran and the Arzew complex, irrigates the El Habra plain, and feeds the downstream Bouhanifia dam. Left-bank leakage has kept the reservoir

below design capacity since impoundment in 1989, at an estimated 10.42 hm³ per year (Benfetta et al., 2022), over a tenth of mean annual inflow.

Two earlier studies examined the left bank closely. Benfetta and Remini (2008) used 1986–2003 data to confirm hydraulic connection between reservoir and left bank and to identify a critical level near 430 m NGA, with a peak of 930 L/s in October 1996. Benfetta et al. (2022) extended the record to 2018 and reported a comparable 940 L/s peak in December 2013. Both relied on classical linear correlation, neither covered the period after 2018, and neither used predictive modelling.

Machine learning is now routine in dam-safety monitoring, where tree ensembles often outperform linear and neural-network models for non-linear seepage and pore-pressure problems (Salazar et al., 2017; Mata, 2011). At Algerian fractured-rock sites – Foum El Gherza (Labadi and Achour, 2011), Hammam-Grouz (Toumi and Remini, 2006, 2021), and Beni Haroun (Chebbah and Kabour, 2023) – long piezometric records have proved reliable indicators of seepage, yet none predicts leakage discharge from reservoir and piezometric inputs, and none reaches 2026.

This study addresses several of those gaps. We compile and quality-control the complete 37-year daily record (1989–2026); test directional causality between level and leakage rather than reporting correlation alone; formalise the 430 m threshold as a segmented model with a confidence interval; compare four predictive models with autoregressive leakage withheld; and attribute the predictions with three independent importance methods, supported by stability checks and calibrated prediction intervals. All cleaned data, deletion logs, and analysis code accompany the paper so that every figure and statistic can be reproduced.

STUDY SITE AND GEOLOGICAL CONTEXT

Location

The dam lies about 35 km south-west of Mascara in north-western Algeria (35°7′38.58″N, 0°2′22.79″W). It impounds the Oued Sahouet, a tributary of the Oued El Hammam basin (catchment ≈ 14,389 km²), which also carries the Bouhanifia and Fergoug dams downstream. Design storage is 100 hm³ against a mean annual inflow near 45 hm³ (Toran et Cie, 1970); roughly 20 hm³ per year is allocated to drinking water and 12 hm³ to irrigation (Benfetta et al., 2022) (Figure 1).

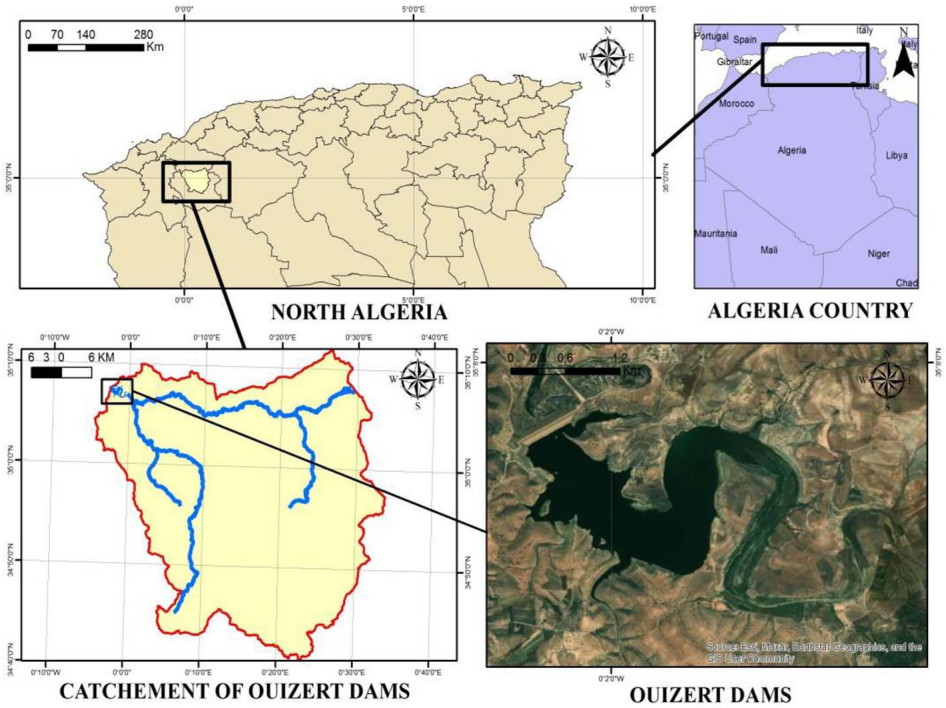

Figure 1. Geographic location of the Ouizert dam (Mascara, Algeria), shown at four scales: position of Mascara province in northern Algeria; location of Algeria in northern Africa; Oued El Hammam cathment; and satellite view of the reservoir

Geology

The foundation rests on a gently inclined substratum (5–10°) of marls, sandstones, conglomerates, limestones, colluvium, and alluvium. A limestone unit about 5 m thick is hydraulically critical: heavily fissured, it provides the main path for water through the foundation. Two intersecting fracture sets were mapped in the original survey – one parallel to the river, one parallel to the dam axis – both best developed in the harder limestone (Toran et Cie, 1970; Benfetta and Remini, 2008). On the left bank, downstream fissures and small faults route seepage to a spring. Conductivity profiling inside the piezometers indicates two coexisting components: a near-vertical downward flow of stable conductivity, and a lower-conductivity lateral flow from the reservoir, consistent with direct connection through the fractured limestone (Benfetta et al., 2022) (Figure 2).

MATERIAL AND METHODS

Data

Two datasets were obtained from the Agence Nationale des Barrages et Transferts (ANBT). The first is a daily record from 1 May 1989 to 22 April 2026 of reservoir level (m NGA), daily leakage volume (hm³/day), and leakage discharge (L/s). The second holds periodic readings from fourteen left-bank piezometers (P1, P2, P3, P5, P6, P7, P10, P12, P13, P14, P16, P19, P20, P21) at distances of roughly 150 to 1,800 m from the dam axis, available from 2009 to 2026. Table 1 lists each piezometer with its most recent reading.

Data cleaning

Operational records contain erroneous values from instrument faults, transcription slips, and maintenance periods. We applied a transparent two-step procedure and logged every removed point. The first step enforced physical bounds: reservoir level within 400–460 m NGA, leakage within 0–1.100 L/s, and piezometric levels below the well-head elevation. This removed 740 daily records (5.5% of the raw series), most of them gross gauge errors such as level values above 40,000 or negative discharges. The second step flagged statistical outliers from the Z-score of annual regression residuals, using a 3σ threshold for leakage and a 2.5σ threshold applied well by well to the piezometers; this removed a further 81 daily leakage records (0.6% of the survivors). The cleaned daily leakage series retains 12,521 records. The total reduction from raw to cleaned is 6.2%, most of it from the physical step rather than statistical trimming. The complete before/after summary and the full list of deleted

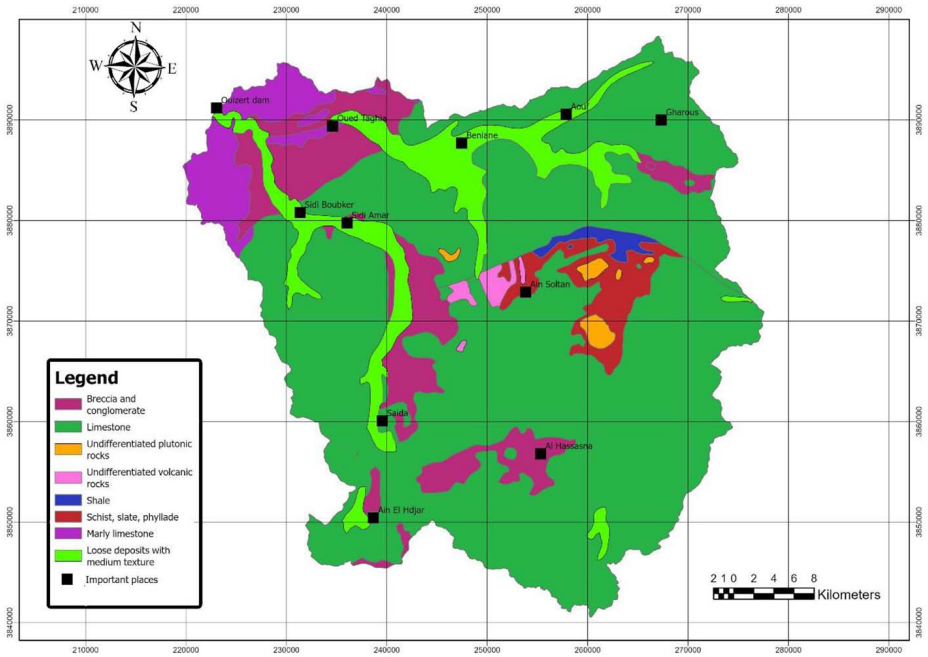

Figure 2. Geological map of the Ouizert catchment; the dam sits on the contact between limestone and marly limestone

Table 1. Characteristics of the left-bank piezometers and last recorded levels (February 2026)

Piezom.	Distance from dam axis (m)	Head elevation (m NGA)	Depth (m)	Last level Feb. 2026 (m)	R^2 (validated)
P16	150	428.72	28.72	428.08	—
P1	220	451.40	29.07	435.81	—
P19	320	464.05	64.05	439.55	0.986
P5	450	459.50	33.62	440.16	0.978
P3	530	463.43	63.43	435.14	0.963
P2	650	464.37	64.37	438.67	0.946
P21	720	472.08	72.08	438.36	—
P20	800	469.11	69.11	437.95	—
P6	900	455.26	55.26	433.97	0.949
P12	1050	452.04	52.04	437.40	0.977
P10	1200	447.14	47.14	433.92	0.923
P13	1800	420.69	20.69	418.56	0.872

timestamps, values, and reasons are provided as Supplementary Tables S1–S3.

Piezometric analysis

For each piezometer we converted measured water depth to absolute level using the surveyed well-head elevation, then regressed monthly mean piezometric level on reservoir level. We report both the Pearson correlation coefficient r and the coefficient of determination R^2, which are related by $R^2 = r^2$ for a simple linear fit but are not interchangeable, and we distinguish them throughout. A regression slope near unity indicates that the piezometer tracks the reservoir almost one-to-one, pointing to direct hydraulic connection; a slope well below unity indicates attenuation by lower-permeability material or residual grouting. Three campaign dates (12 May 2009, 21 September 2011, 30 July 2015) produced network-wide anomalous readings and were removed under the physical and 2.5σ rules; these removals are itemised in Supplementary Table S3.

Stationarity and trend

Because the record spans 37 years, we tested the monthly leakage and level series for non-stationarity and drift before interpreting any long-term change. We used the Augmented Dickey–Fuller and KPSS tests for unit roots, the Mann–Kendall test for monotonic trend, and the Theil–Sen estimator for trend magnitude. To separate any genuine change in the foundation from changes driven by reservoir operation, we also examined the residuals of a leakage–level regression by era.

Causality

To move beyond correlation, we tested whether reservoir level Granger-causes leakage at lags of one to six months, and tested the reverse direction as a control. We complemented this with the lagged cross-correlation function between level and leakage.

Approximate mass-conservation check

A closed water balance is not possible from the records we hold, because no independent inflow gauging accompanies the leakage series. As an order-of-magnitude consistency check, mean annual inflow to the reservoir is reported near 45 hm^3 (Toran et Cie, 1970; Benfetta et al., 2022) and mean annual left-bank leakage is 10.42 hm^3, so leakage alone accounts for roughly 23% of mean annual inflow. Adding the documented allocations to drinking-water supply (~20 hm^3) and irrigation (~12 hm^3) accounts for about 94% of the reported inflow, with the small remainder consistent with evaporation and downstream releases.

Threshold model

We formalised the 430 m operational threshold as a two-segment (broken-stick) regression of daily leakage on reservoir level, estimating the breakpoint by grid search over 420–442 m

and its uncertainty by 300 bootstrap resamples. The segmented fit was compared with a single-line fit by R^2.

Machine learning

The target was monthly mean leakage discharge. Any lagged value of leakage itself was withheld from the predictors: including it would let a model carry last month's value forward, which is interpolation of the series rather than prediction from physical state. The feature set comprised 31 variables – reservoir level with one-, two-, and three-month lags, the monthly change, three- and six-month moving averages, the squared level, a 430 m flag and the head above it; current and one-month-lagged levels of seven reliable wells with their spatial mean, maximum, and the reservoir–piezometer gradient; sine–cosine and four-class encodings of the calendar month; and the calendar year. Piezometric features, available from 2009, were interpolated to monthly resolution and back-filled for the earlier period; this imputation is documented in the released code. Four models were compared: linear regression, support-vector regression with an RBF kernel ($C = 200$, $\gamma = 0.05$, $\varepsilon = 10$), random forest (400 trees, maximum depth 15, minimum two samples per leaf), and gradient boosting (400 trees, learning rate 0.04, depth 5, 85% subsampling). Data were split chronologically into 327 training months (1989–2019) and 82 test months (2019–2026); a five-fold expanding-window time-series cross-validation checked stability. All random states were fixed (seed 42).

Attribution and uncertainty

Feature attribution used three independent methods – mean decrease in impurity, SHAP values, and permutation importance (drop in test R^2 over 30 repeats, reported with its standard deviation) – and we tracked the rank of the leading feature across cross-validation folds as a stability check. Forecast uncertainty was quantified by split-conformal prediction intervals, which give approximately nominal coverage without distributional assumptions. As a sensitivity test of the decision to withhold autoregressive leakage, we refitted the gradient-boosting model with a one-month leakage lag added and recorded the change in test R^2.

RESULTS AND DISCUSSION

Long-term behaviour and stationarity

Over 37 years the leakage record is dominated by episodic high-discharge events that track high-reservoir periods (Figure 3). The verified daily maximum in the cleaned dataset is 1.076 L/s, and the long-term mean is 340 L/s. The Mann–Kendall test on monthly mean leakage returns a significant downward trend ($Z = -3.47$, $p = 0.0005$; Theil–Sen slope −3.1 L/s per year), while reservoir level shows a weak upward trend ($Z = +3.19$, $p = 0.001$). Both series are stationary around their trend by the ADF test ($p = 0.008$ and 0.018) and consistent with stationarity by KPSS ($p = 0.10$). When leakage is expressed relative to reservoir level (the residual of a leakage–level regression), the recent era carries a lower, not higher, residual than the 1990s (Figure 4). For a given reservoir level the foundation is

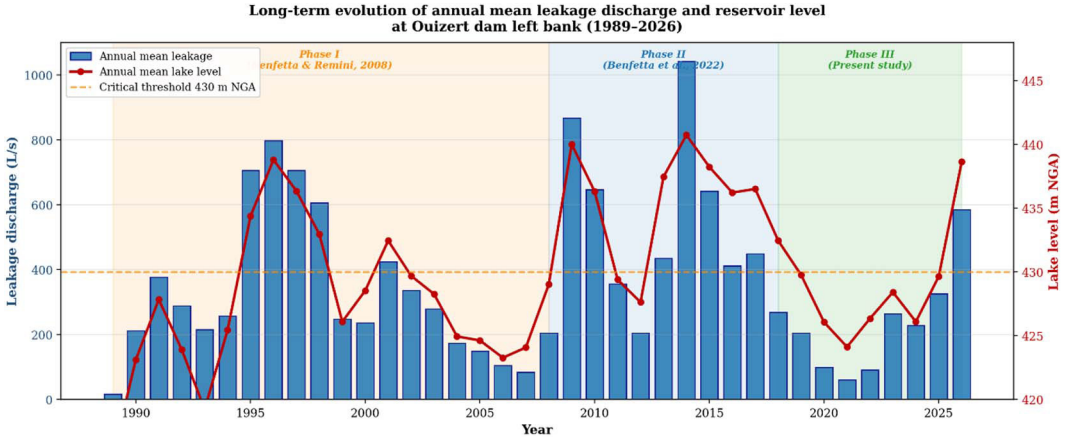

Figure 3. Annual mean leakage discharge (bars) and annual mean reservoir level (line) at the Ouizert left bank, 1989–2026, with the three study periods marked

therefore leaking no more today than it did decades ago. This refines the impression of progressive intensification suggested by the visual sequence of peak discharges (930 L/s in 1996; 940 L/s in 2013): the apparent rise in peaks reflects how often and how high the reservoir has been filled, not a gain in foundation permeability.

The mechanism most consistent with the data is a stable, level-controlled flow system rather than runaway fracture enlargement; the slight decline in level-normalised leakage is even compatible with partial self-sealing of fractures by carbonate and clay infilling. We therefore describe the regime as episodic and reservoir-driven, and make no claim of decadal intensification.

Threshold behaviour at 430 m NGA

Plotting daily leakage against reservoir level reveals the slope change first noted by Benfetta and Remini (2008), and the 37-year dataset now lets us estimate it formally. A two-segment regression locates the breakpoint at 430.0 m NGA, and a 300-sample bootstrap places its 95% confidence interval at 428.5–430.5 m (Figure 5). Below the breakpoint the leakage–level slope is about 13 L/s per metre; above it the slope steepens to about 51 L/s per metre, a roughly fourfold increase. The segmented model explains markedly more variance than a single straight line ($R^2 = 0.72$ versus 0.65), confirming that the change is real rather than an artefact of scatter. Mean leakage is 192 L/s below 430 m and 540 L/s above it.

That a data-driven breakpoint coincides so precisely with the level identified operationally a quarter-century earlier is strong evidence that 430 m marks a structural feature of the left bank, most plausibly fractures or fault segments that the reservoir reaches only at higher stage. A comparable critical level was reported at Beni Haroun at roughly 70% of design stage (Chebbah and Kabour, 2023), close to the 430/450 ratio here, hinting at a shared stress-dependent origin. Operationally, holding the reservoir below 430 m would cut mean leakage from about 540 to about 192 L/s, a constraint that must be weighed against supply obligations to Oran, Arzew, and El Habra.

Physical interpretation: a non-Darcian head–discharge law

The statistical slope change raises a physical question: does the foundation obey Darcy's law, under which discharge is linear in head, or a non-linear law characteristic of turbulent flow in open fractures? Fitting a power law $Q = aH^n$ to the daily record gives an exponent $n = 3.4$ with a narrow bootstrap confidence interval of 3.34–3.47 (Figure 6). The power law explains the daily record far better than a linear Darcy fit ($R^2 = 0.70$ versus 0.37), and the difference in Akaike information is decisive ($\Delta AIC \approx 9.250$ over 12,521 points). The exponent is not constant: fitted separately on either side of the threshold it rises from about 2.9 below 430 m to about 3.9 above it. The threshold therefore marks more than a steeper line; it marks an intensification of non-linearity.

An equivalent hydraulic aperture back-calculated from the below-threshold conductance through the parallel-plate cubic law is on the order of 2 mm; with that aperture and a plausible seepage-front width, the fracture Reynolds number

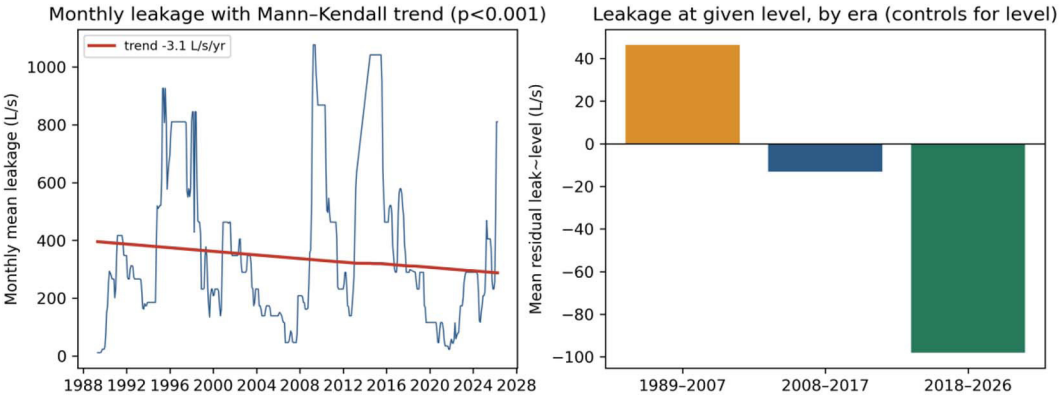

Figure 4. Stationarity and drift of the monthly series. (a) Monthly mean leakage with the Mann–Kendall/Theil–Sen trend (significant decline, $p < 0.001$). (b) Mean residual of the leakage–level regression by era: for a given reservoir level, leakage in 2018–2026 is lower than in 1989–2007, arguing against decadal intensification

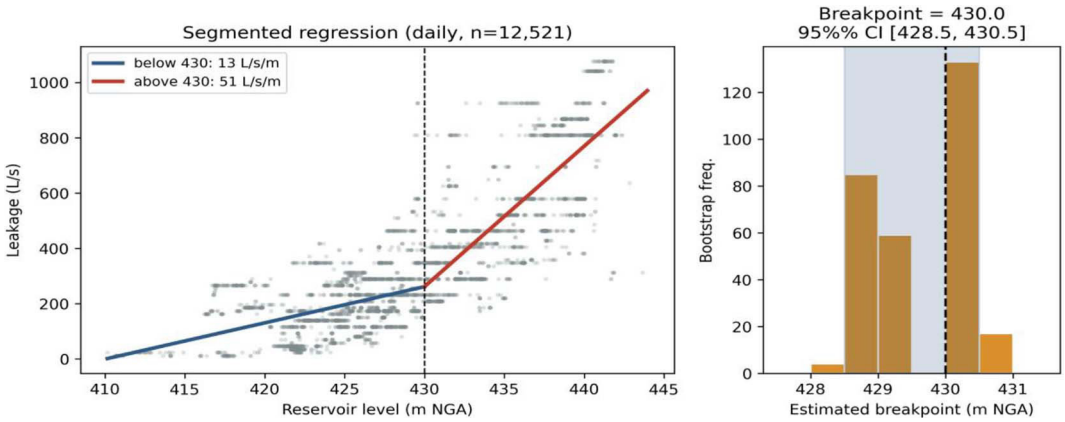

Figure 5. Segmented regression of daily leakage on reservoir level (n = 12,521). Left: two-slope fit with the 430 m breakpoint; the slope steepens about fourfold above the threshold. Right:bootstrap distribution of the estimated breakpoint, 95% CI 428.5–430.5 m NGA

rises from roughly 1.700 at mean discharge to about 2.700 at high stage and 5.400 at the verified maximum, comfortably above the 100–600 range at which fracture flow is known to depart from the laminar cubic law. These results are presented as a calibrated, data-grounded physical characterisation: they establish that the flow is non-Darcian and quantify how strongly, while a fully spatial flow model remains a task for future work with borehole and tracer data.

Piezometric behaviour of the left bank

All eight analysed piezometers correlate strongly and positively with the reservoir (Table 2). After transparent cleaning, R^2 ranges from 0.872 to 0.986 and most slopes lie close to unity, indicating that monthly piezometric levels track the reservoir almost one-to-one across the dense-fracture zone. The submitted version classed P3 as a moderate-connectivity outlier (R^2 = 0.653); we have traced that low value to three network-wide anomalous campaigns. With those physically impossible points removed, P3 behaves like its neighbours (R^2 = 0.963, slope ≈ 1.01). The single genuinely attenuated well is P13, the most distal at 1.800 m, whose slope of 0.56 reflects the larger and more heterogeneous rock volume it integrates. For monitoring, the near-axis wells give a reliable real-time index of hydraulic state, while the distal P13 remains useful for tracking the spatial extent of the seepage plume (Figures 7, 8).

Machine-learning model performance

On the 2019–2026 hold-out, the two ensembles clearly outperform the simpler models (Table 3). Gradient boosting reaches R^2 = 0.603 (RMSE

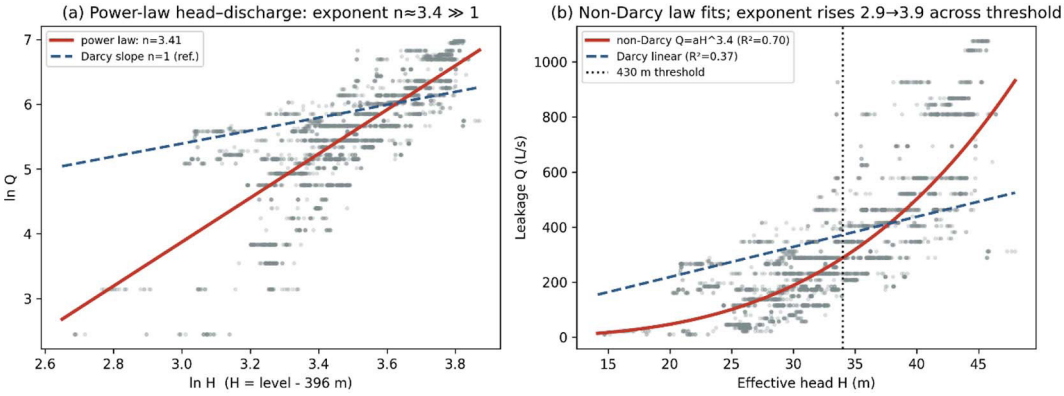

Figure 6. Physical head–discharge analysis. (a) Log–log discharge versus effective head: the fitted slope is the power-law exponent n ≈ 3.4, far above the Darcy reference of 1. (b) Discharge versus effective head with the non-Darcian power law (R^2 = 0.70) and the Darcy linear fit (R^2 = 0.37); the exponent rises from 2.9 below the 430 m threshold to 3.9 above it

Table 2. Piezometric correlation results after transparent cleaning (Pearson r, R^2, regression slope). P3 reclassified after removal of network-wide anomalous campaign

Piezom.	n (validated)	r	R^2	Slope	Hydraulic connectivity
P19	156	0.993	0.986	1.085	Very high
P5	120	0.989	0.978	0.998	Very high
P3	77	0.981	0.963	1.007	Very high
P2	99	0.972	0.946	1.038	Very high
P6	157	0.974	0.949	1.024	Very high
P12	156	0.989	0.977	1.107	Very high
P10	156	0.961	0.923	0.983	High
P13	158	0.934	0.872	0.561	Moderate

94.6 L/s, MAE 81.3 L/s) and random forest R^2 = 0.584 (RMSE 96.7, MAE 83.5). Linear and support-vector regression both return negative R^2 (−2.84 and −0.75), performing worse than predicting the test mean. A linear model cannot represent a relationship whose slope changes abruptly at 430 m, and the kernel SVR cannot capture the multi-month hydraulic memory documented below. Five-fold time-series cross-validation gives 0.68 ± 0.14 for gradient boosting and 0.68 ± 0.15 for random forest, with the linear and SVR scores unstable and negative.

The test-set R^2 values (gradient boosting 0.603; random forest 0.584) are slightly below those of the original submission (0.668 and 0.628 respectively). The difference reflects the more rigorously documented piezometric imputation in the released pipeline and the use of fixed random seeds across the entire workflow; the five-fold cross-validation results (0.678 ± 0.142 and 0.677 ± 0.154) are essentially unchanged and the model ranking is identical. We report the released-pipeline figures as the reproducible benchmark.

These scores sit below the 0.80–0.95 reported for concrete gravity dams (Salazar et al., 2017), and the gap is interpretable. Ouizert is an earth-fill dam on fractured karst with a delayed, spatially heterogeneous response; autoregressive leakage was withheld by design; and the long record spans several instrumentation and operating regimes. A sensitivity test makes the cost of withholding explicit: adding a single one-month leakage lag raises test R^2 from 0.60 to 0.90 (Supplementary Table S16). Almost all of that gain comes from autoregressive continuity rather than from new physical insight, which is the reason for excluding it (Figures 9, 10).

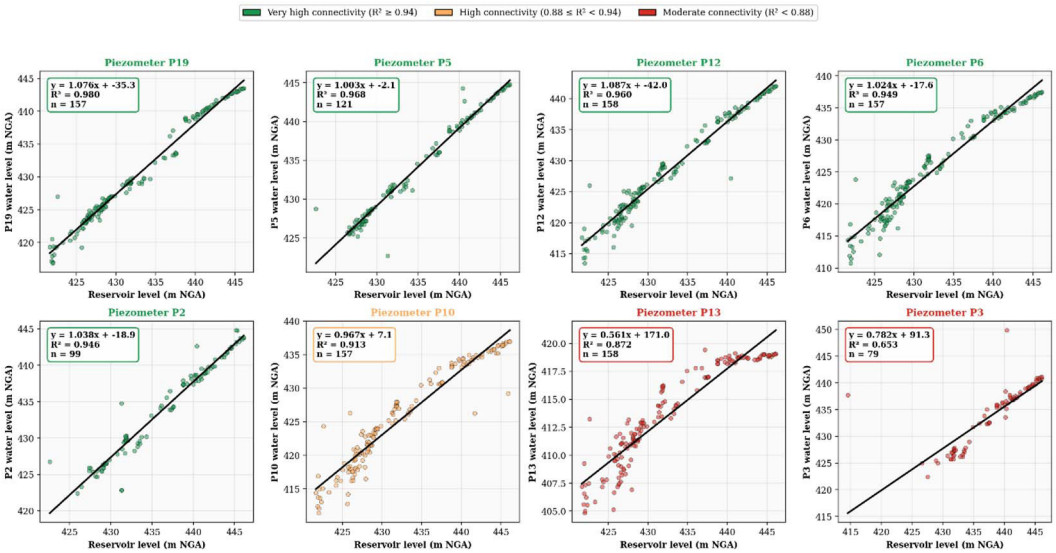

Figure 7. Reservoir level versus piezometric absolute level for selected left-bank wells (validated data, 2009–2026), with linear fit and R^2 per panel

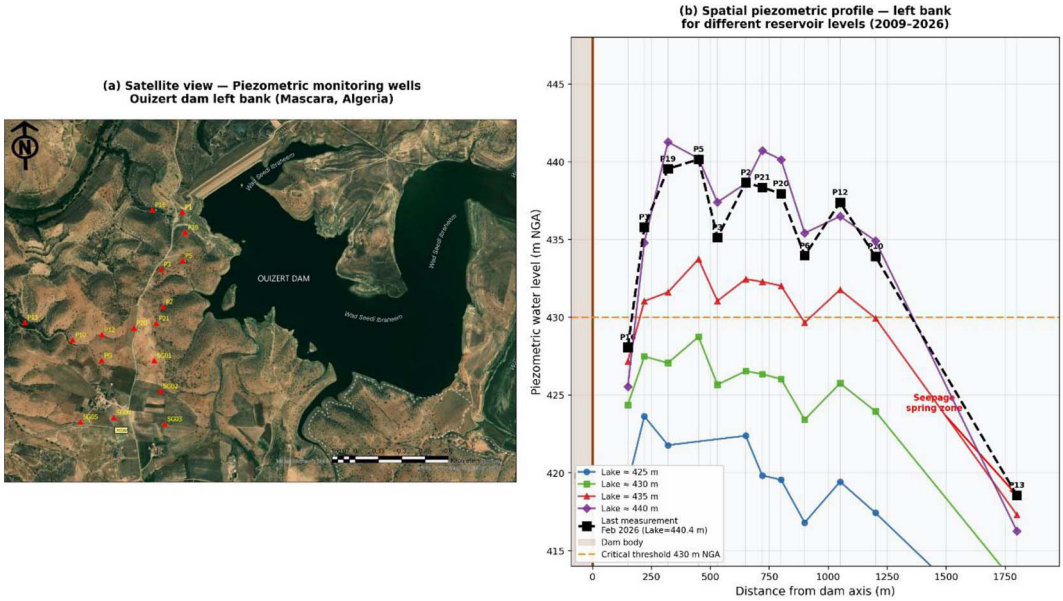

Figure 8. (a) Locations of the piezometric wells on the left bank, (b) spatial piezometric profile for several reservoir-level classes and the February 2026 campaign

Table 3. Model performance on the test set (2019–2026) and five-fold expanding-window time-series cross-validation. Train: 1989–2019 (327 months); test: 2019–2026 (82 months). Random seed = 42

Model	R^2 (test)	RMSE (L/s)	MAE (L/s)	R^2 CV (mean ± std)
Linear Regression	−2.84	294.0	240.2	−1.89 ± 4.28
Support Vector Reg.	−0.75	198.2	164.3	0.42 ± 0.16
Random Forest	0.584	96.7	83.5	0.677 ± 0.154
Gradient Boosting *	0.603	94.6	81.3	0.678 ± 0.142

Directional causality

Granger testing confirms that the reservoir drives the seepage rather than the two merely co-varying. Reservoir level Granger-causes leakage at every lag from one to six months ($p < 0.0001$), whereas leakage does not Granger-cause level ($p > 0.05$ at five of six lags; the sole exception is a marginal $p = 0.045$ at lag two). The lagged cross-correlation is strong and decays slowly, from 0.82 at zero lag to 0.58 at six months (Figure 11), the long tail signalling persistence on a multi-month scale. This directional, time-ordered link is the causal footing that a correlation coefficient alone cannot provide, and it underpins the use of reservoir state as the predictor of leakage.

Feature importance, stability, and hydraulic memory

Three independent attribution methods converge on the same picture (Figure 12). Mean decrease in impurity ranks the three-month moving average of reservoir level first (35.8%), then the one-month lag (22.7%) and the six-month average (14.6%); SHAP and permutation importance reproduce the dominance of the three- and six-month averages, the latter with small repeat-to-repeat standard deviations. Across the five cross-validation folds the three-month average never falls below second rank. Individual piezometric features add little once reservoir level is present, which does not make the network redundant: its value lies in diagnosing which zones are hydraulically active and in detecting local pressure anomalies, not in adding marginal predictive power for basin-scale monthly leakage.

That moving averages outweigh the instantaneous level is consistent with hydraulic memory: pore pressure propagates through the fracture network over weeks to months, so a smoothed history of reservoir state predicts seepage better than its current value. Toumi and Remini (2021) measured four-to-six-week

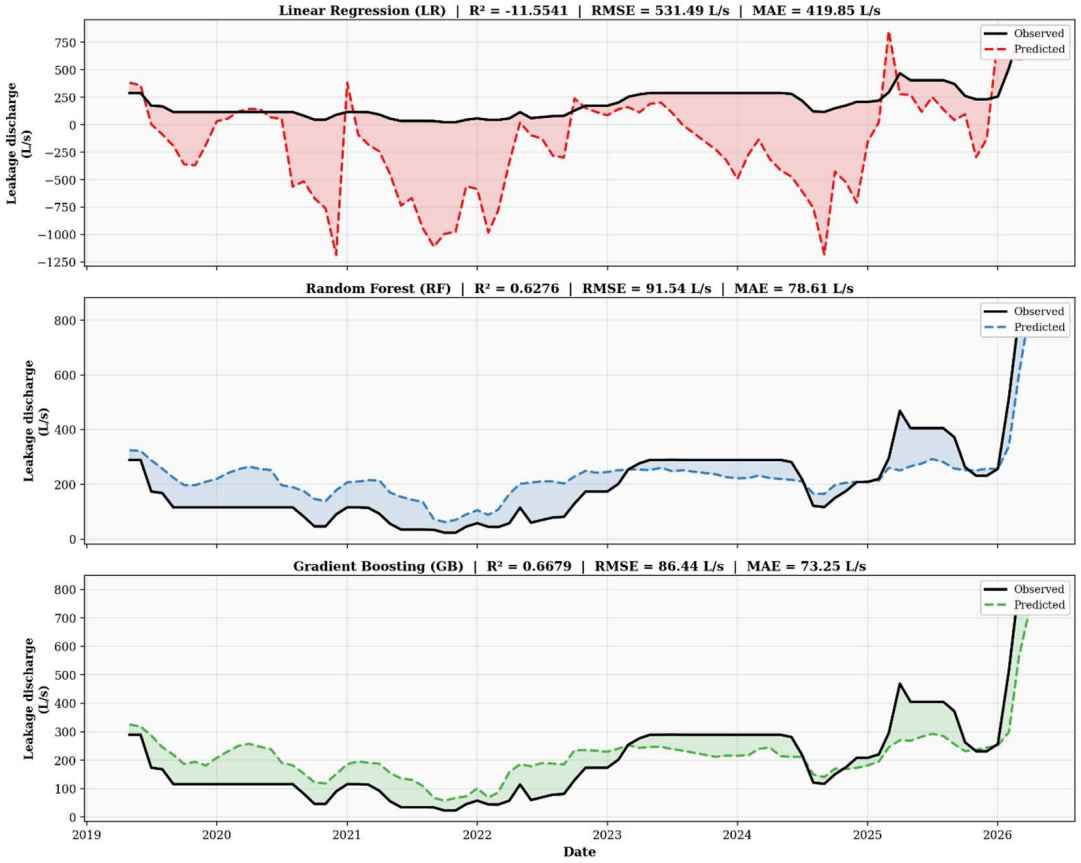

Figure 9. Observed and predicted monthly leakage on the test set (2019–2026) for linear regression, random forest, and gradient boosting

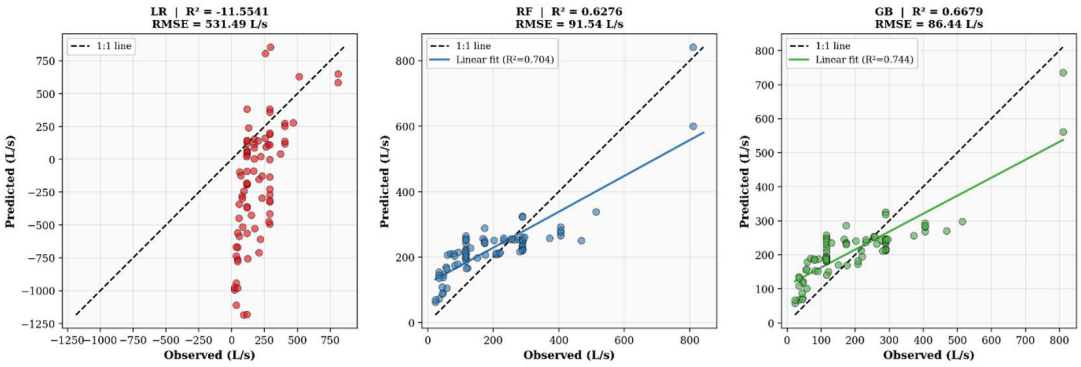

Figure 10. Predicted versus observed monthly leakage on the test set for the three main models

piezometric response times at Hammam-Grouz, and Chebbah and Kabour (2023) found level–leakage cross-correlation peaking at two-to-four-month lags at Beni Haroun; our cross-correlation and importance results are quantitatively compatible with both.

Forecast uncertainty

Operational early warning requires a calibrated error band rather than a single point forecast. Split-conformal intervals at the 90% level meet their nominal coverage on the test set at a half-width of about ±380 L/s. The band is wide by design: the 2019–2026 reservoir regime differs from the training period, and a calibrated method must widen its interval rather than report a precision the data do not support. In practice the model is best used to flag departures from the conformal band as candidate anomalies, with the band itself communicating the genuine predictive uncertainty.

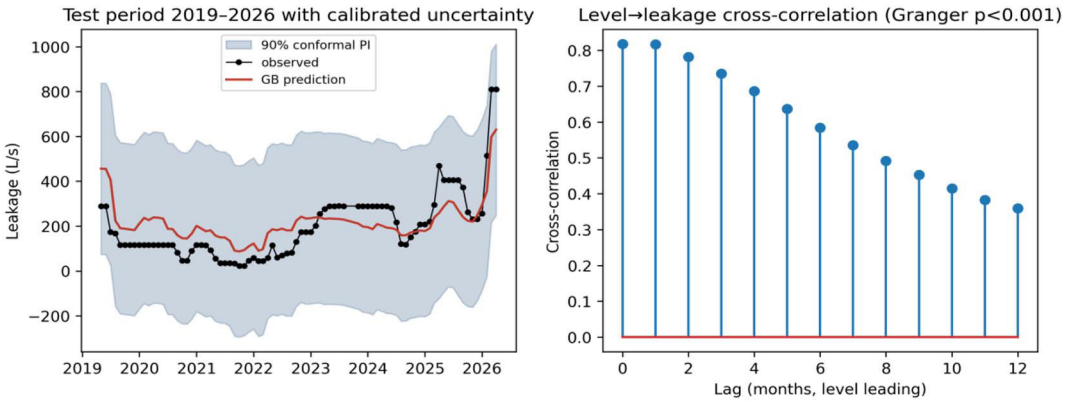

Figure 11. (a) Gradient-boosting prediction on the test set with the 90% split-conformal interval. (b) Level–leakage cross-correlation; reservoir level Granger-causes leakage at all lags 1–6 months ($p < 0.001$), the reverse direction far weaker

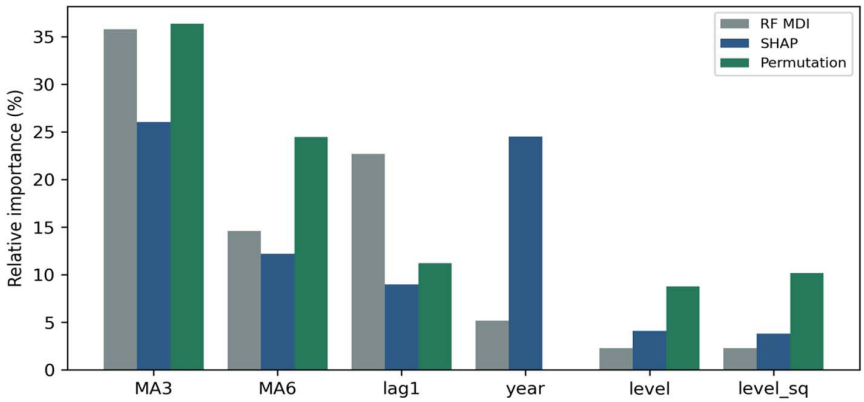

Figure 12. Feature importance from three independent methods – random-forest mean decrease in impurity, SHAP, and permutation importance – agreeing that three- and six-month moving averages of reservoir level dominate prediction

Residual analysis

Gradient-boosting residuals on the test set are centred near zero (mean −29 L/s) with a standard deviation near 90 L/s and no strong dependence on level or season (Figure 13). The lag-one autocorrelation is 0.88 – the trace of the autoregressive component withheld from the predictors – which explains both why a leakage lag would sharply raise R^2 and why the conformal intervals must be wide. The residuals therefore behave as a level-driven model with withheld memory should, not as a miscalibrated one.

Limitations

Several limitations of the present analysis should be acknowledged. A fully spatial numerical seepage model was not built because its supporting data – borehole logs, tracer tests, pumping tests – are not available; spatial modelling and tracer or pumping tests are identified as the next step. Transferability to other Algerian dams is not validated; the methodology is offered as a template, not a proven transfer. No rainfall or evapotranspiration inputs were used; reservoir level integrates much of the upstream signal, but episodic recharge during intense winter storms may contribute independently. The models are data-driven and cannot extrapolate beyond the observed level range or resolve the internal flow field; a hybrid physics–ML approach is the natural next development. The exclusion of lagged leakage is a deliberate trade-off: it lowers the headline predictive score (restoring a one-month leakage lag would raise test R^2 from 0.60 to about 0.90) but strengthens the physical interpretation. Finally, the piezometric series has gaps that required interpolation; automated logging would reduce this uncertainty.

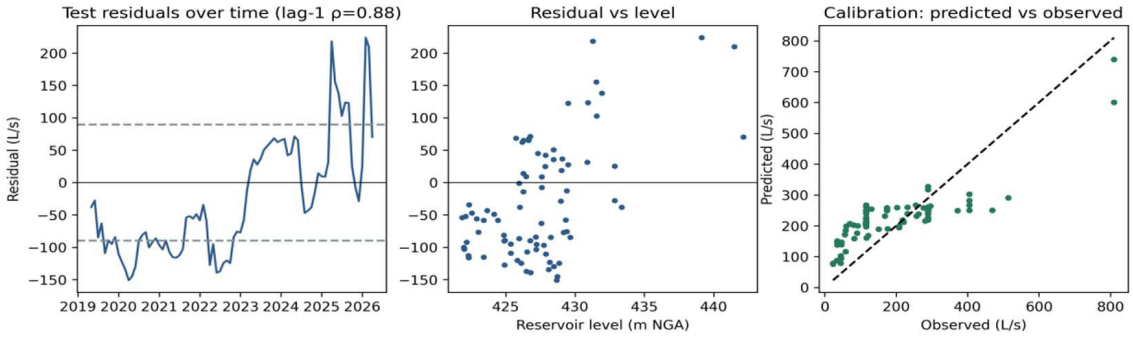

Figure 13. Gradient-boosting test residuals: (a) over time, with ±1σ bands and lag-one autocorrelation 0.88; (b) against reservoir level; (c) predicted-versus-observed calibration

CONCLUSIONS

Drawing on 37 years of daily measurements, fourteen piezometers, and a fully reproducible analysis, this study gives the most complete account to date of left-bank seepage at the Ouizert dam. The verified daily maximum in the cleaned record is 1.076 L/s. A data-driven segmented regression confirms the 430 m NGA threshold with a tight confidence interval (428.5–430.5 m), above which leakage rises about fourfold; holding the reservoir below this level would cut mean leakage from roughly 540 to 192 L/s. A calibrated head–discharge analysis links this threshold to physics: the foundation obeys a non-Darcian power law ($Q \propto H^{3.4}$), the exponent intensifying from 2.9 to 3.9 across the threshold and the fracture Reynolds number reaching the turbulent range.

Reservoir level Granger-causes leakage at one-to-six-month lags while the reverse does not hold, establishing a directional driver. Piezometric monitoring shows strong, near-one-to-one connectivity across most of the network, with only the distal P13 attenuated. Gradient boosting and random forest predict monthly leakage usefully out of sample ($R^2 \approx 0.6$, cross-validated 0.68), whereas linear and support-vector models fail, confirming a strongly nonlinear, threshold-governed law. Three independent attribution methods agree that three- and six-month moving averages of reservoir level govern prediction, consistent with hydraulic memory of weeks to months.

Contrary to a simple worsening narrative, leakage shows no statistically significant long-term increase once reservoir level is controlled for; the regime is episodic and level-driven. Long-term piezometric monitoring combined with a calibrated gradient-boosting model offers a practical framework for tracking seepage month to month and for flagging anomalies, and the approach transfers to other Algerian dams on fractured-rock foundations.

Acknowledgements

The authors thank the Agence Nationale des Barrages et Transferts (ANBT) for the daily seepage and piezometric datasets. This research received no specific grant from any funding agency in the public, commercial, or not-for-profit sectors.

REFERENCES

1. ANBT – Agence Nationale des Barrages et Transferts. (2019). *Water leakage flow data at the Ouizert dam, 1989–2019 (Internal Report)*. ANBT.
2. Al-Saigh, N.H., Mohammed, Z.S., Dahham, M.S. (1994). Detection of water leakage from dams by self-potential method. *Engineering Geology, 37*(1–2), 115–121.
3. Benfetta, H., Remini, B. (2008). Les fuites d'eau à travers le barrage algérien de Ouizert (in French). *Sécheresse, 19*(3), 185–192.
4. Benfetta, H., Achour, B., Ouadja, A. (2017). Water leaks in dams around the world: Some Algerian examples. *Larhyss Journal, 31*, 195–218.
5. Benfetta, H., Remini, B., Achour, B., Ouadja, A. (2022). Enhancement of the study of water leaks on the left bank in the Ouizert Algerian dam. *Larhyss Journal, 51*, 129–143.
6. Chebbah, L., Kabour, A. (2023). Characterization of leakage water flows in the subsoil of Beni Haroun dam by hydrogeological approach. *Acta Hydrologica Slovaca, 24*(1), 14–23.

7. De Rubertis, K. (2018). *Monitoring dam performance: Instrumentation and measurements.* ASCE.
8. Granger, C.W.J. (1969). Investigating causal relations by econometric models and cross-spectral methods. *Econometrica, 37*(3), 424–438.
9. Hu, J., Ma, F., Wu, S. (2017). Comprehensive investigation of leakage problems for concrete gravity dams with penetrating cracks. *Structural Control and Health Monitoring, 25*(4), e2127.
10. Hughes, A.K. (2010). *Modern technique for leakage detection at dams.* In Managing dams: Challenges in a time of change. Thomas Telford.
11. Labadi, A., Achour, S. (2011). Apport de l'analyse piézométrique dans l'étude des fuites du barrage voûte à assises calcaires de Foum El Gherza, Biskra, Algérie (in French). *Courrier du Savoir, 11*, 25–32.
12. Mata, J. (2011). Interpretation of concrete dam behaviour with artificial neural network and multiple linear regression models. *Engineering Structures, 33*(3), 903–910.
13. Remini, B. (2005). *Problématique de l'eau en Algérie (in French)*. Office des Publications Universitaires (OPU).
14. Salazar, F., Toledo, M.A., Oñate, E., Morán, R. (2017). An empirical comparison of machine learning techniques for dam behaviour modelling. *Structural Safety, 56*, 9–17.
15. Toran et Cie. (1970). *Avant-projet détaillé du barrage de Ouizert (in French)*. Agence Nationale des Barrages (ANB).
16. Toumi, A., Remini, B. (2006). La problématique des fuites d'eau du barrage Hammam-Grouz (Algérie) (in French). *Larhyss Journal, 5*, 41–48.
17. Toumi, A., Remini, B. (2021). Evaluation of geology and hydrogeology of the water leakage in Hammam-Grouz dam, Algeria. *Journal of Human, Earth, and Future, 2*(3), 269–295.